Synthesis and Molecular Docking Study of Benzimidazole-Triazole Derivatives as Antifungal Agents

¹Zahra Maryam, ¹Ulviye Acar Çevik*, ²Ravikumar Kapavarapu, ^{3,4}Emir Güzel, ⁵Uğur Kayış, ⁶Ülküye Dudu Gül, ¹Yusuf Özkay and ¹Zafer Asım Kaplancıklı ¹Department of Pharmaceutical Chemistry, Faculty of Pharmacy, Anadolu University, Eskişehir 26470, Turkey.

²Department of Pharmaceutical Chemistry and Phytochemistry, Nirmala College of Pharmacy, Atmakur, Mangalgiri, Guntur district, Andhra Pradesh, India.

³Department of Pharmaceutical Chemistry, Graduate School, Anadolu University, Eskişehir 26470, Turkey. ⁴Health Vocational School, Program of Pharmacy Services, Nişantaşı University, 34406 İstanbul, Turkey. ⁵Pazaryeri Vocational School, Program of Pharmacy Services, Bilecik Şey Edebali University, 11230 Bilecik, Turkey.

⁶Department of Bioengineering, Faculty of Engineering, Bilecik Seyh Edebali University, Bilecik, Turkey. <u>uacar@anadolu.edu.tr*</u>

(Received on 9th October 2023, accepted in revised form 3rd December 2024)

Summary: Drugs comprising benzimidazole-triazole structure have become increasingly clinically significant in recent years, making them more efficient scaffolds in medicinal chemistry. Due to their numerous biological characteristics, these moieties have gained tremendous attention. The objective of the current study was to effectively synthesize a new series of benzimidazole-triazole analogues. Within the scope of this study, potential benzimidazole-triazole derivatives (7a–7e) were synthesized according to the methods we used before and antifungal activity tests were performed. The structures of these hybrids were elucidated using NMR, mass spectrometry, and elemental analysis. Then the antifungal activity of these hybrid compounds were tested *in-vitro* against *Candida krusei*, *Candida albicans*, *Candida glabrata*, and *Candida parapsilopsis*. Compounds 7a and 7b showed highest activity, with 0.97 μ g/ml minimum inhibitory concentration. Then evaluation of the molecular interactions between compounds 7a and 7b and the fungal cytochrome P450 lanosterol 14α -demethylase protein was performed using *in silico* docking simulations. To demonstrate the new compounds' druggability, *in-silico* pharmacodynamics and ADMET characteristics were also performed. The findings of this study suggest that the compounds 7a and 7b could be useful leads for the development of new 14α -demethylase inhibitors.

Keywords: Benzimidazole, Triazole, Antifungal, Molecular docking, 14α -demethylase.

Introduction

Infectious diseases brought on by microbes, particularly bacteria and fungi impose significant hazard to human health. The hazard to human health from fungal infections has increased significantly over the past few decades. An estimated 1.5 to 2 million people per vear die from fungi-related diseases. Currently, five different chemical classes are used to treat and prevent fungal diseases in different parts of the world: polyenes, acrylamines, antimetabolites, and echinocandins. However, the treatment of numerous microbial diseases has been severely hampered by the overuse, broad usage, and abuse of antimicrobials [1-2]. Moreover, despite the largest advancements in microbial therapy, the current treatment has some serious drawbacks, such as drug resistance, nonspecificity of drugs, and high levels of toxicity [2-5]. All these factors necessitate the research for new antimicrobials and ongoing research to develop new and improved antimicrobial medications continues to be a crucial indicator in medicinal chemistry. In medicinal chemistry, heterocyclic compounds play a key role as therapeutics for most diseases. Among these heterocycles, triazole/imidazole/benzimidazole derivatives are favoured building blocks for the synthesis of novel pharmaceuticals. In this research, triazole/benzimidazole skeleton containing compounds were designed, synthesized, and then biological activity of these hybrid compounds were determined [6-7].

Benzimidazole stands out among these heterocycles and has pharmacophore that is analogous to purine with a wide range of therapeutic action [8-9]. Due to its crucial significance in medicinal chemistry, benzimidazole derivatives have attracted a lot of interest in synthesis and bioassay studies. Benzimidazole is formed by joining benzene ring to an imidazole, which has two nitrogen atoms at the neighbouring site. Benzimidazoles, the most significant class of systemic fungicides, are eminent for their antifungal potential [10]. The other skeleton

for our research, 1,2,3-triazoles, are well-known conjugational scaffolding with benzimidazole. This scaffold, the triazole ring, a special pharmacophore, serves as antimalarial [11], antiviral antibacterial, as well as antifungal agent [13]. Triazole rings' improved biological activities are due to its moderate dipole qualities, hydrogen bonding ability, and rigidity [14]. The heterocyclic nitrogen atom on benzimidazole, and triazole ring allows azoles to coordinate to the haem iron in the active site and block α-demethylase enzyme [15]. Numerous discussions and reviews have been conducted regarding the efficacy of the pharmacological target sterol 14-demethylase (CYP51) in preventing the growth and replication of fungi. The drugs containing azole ring structure (benzimidazole, and triazole) target 14α-demethylase and are termed as demethylase inhibitors (DMIs). This 14αdemethylase, CYP51, member of cytochrome P450 family, a hemoprotein, facilitates the three-step oxidative removal of the 14-methyl group from cyclised sterol precursors, which results in the formation of ergosterol, which is essential for maintaining the integrity of cell membranes and serves as a metabolic precursor to several signalling molecules [16]. Azole drugs block this enzyme, and this hampers the integrity of fungal cell membrane.

Ulviye et al. therefore deemed it valuable to synthesize some new chemical entities having benzimidazole and 1,2,3-triazole moieties to understand the combined effect of both benzimidazole and 1,2,3-triazole structures. These structures entail a single molecular framework housing many pharmacophores in one molecule. In previous studies, promising antifungal activity was obtained with benzimidazole-triazole structure [17-19]. Following the effective synthesis of the compounds, structural analysis of these compounds was performed by spectroscopic methods to confirm the benzimidazole-triazole structures. Then we tested their effectiveness of the synthesized compounds against four fungal strains C. krusei (ATCC 6258), C. albicans (ATCC 24433), C. glabrata (ATCC 9), and C. parapsilopsis (ATCC 22019). Voriconazole and fluconazole were employed as standard reference drugs.

Experimental

Chemistry

General

All of the chemicals used in the synthetic process were obtained from Merck Chemicals

(Merck KGaA, Darmstadt, Germany) or Sigma-Aldrich Chemicals (Sigma-Aldrich Corp., St. Louis, MO, USA). The uncorrected melting points of the compounds that were obtained were ascertained using the MP90 digital melting point instrument (Mettler Toledo, OH, USA). Using a Bruker 400 MHz and 100 MHz digital FT-NMR spectrometer (Bruker Bioscience, Billerica, MA, USA), the produced compounds' ¹H-NMR and ¹³C-NMR spectra were recorded in DMSO-d₆, respectively. Here are the designated splitting patterns: NMR spectra with the following symbols: s: singlet, d: doublet, t: triplet, and m: multiplet. The unit of measurement for coupling constants (J) was Hertz. The Shimadzu LC/MSMS system (Shimadzu, Tokyo, Japan) was used to determine the M+1 peaks. Thinlayer chromatography (TLC) was used to track all reactions using Silica Gel 60 F254 TLC plates (Merck KGaA, Darmstadt, Germany).

General procedure for acetylation of aniline derivatives (1a-1e)

In an ice bath, the appropriate aniline derivatives (25 mmol) and TEA (30 mmol, 4.23 mL) were combined with 75 ml of THF. To this solution, drops of chloroacetyl chloride (30 mmol, 2.4 mL) in THF (10 mL) were added. The reaction mixture was then stirred for 1 hour at room temperature. The precipitated product underwent filtering, a water wash, drying, and recrystallization from ethanol.

Synthesis of sodium metabisulfite salt of benzaldehyde derivative (2)

First of all, in ethanol, methyl 4-formyl benzoate (2.5g, 0.015 mol) was dissolved. Sodium metabisulfite (3.42 g, 0.018 mol) dissolved in ethanol was added dropwise into the benzaldehyde solution. After completing the dripping procedure, the reaction's components were combined and allowed to sit at room temperature for an hour. The precipitated product was filtered out.

Synthesis of 4-(5-cyano-1H-benzimidazol-2-yl) benzoic acid methyl ester (3)

After dissolving 5-cyano-1,2-phenylenediamine (0.011 mol) in DMF, a benzaldehyde derivative (3.55 g, 0.013 mol) salt of sodium metabisulfite was added. The final product was precipitated by adding the ingredients of the reaction to freezing water. The precipitated product was then extracted and crystallized from the ethanol.

Synthesis of 4-(5-cyano-1H-benz[d]imidazol-2-yl) benzohydrazide (4)

Compound 3 (0.009 mol) and excess of hydrazine hydrate (2.5 mL) were dissolved in ethanol (7.5 mL). The mixture refluxed for 12 hours. After the reaction was complete, the liquid was submerged in freezing water, and the resulting product was filtered.

Synthesis of 2-(4-(5-cyano-1H-benz[d]imidazol-2-yl) benzoyl)-N-phenylhydrazine-1-carbothioamide (5)

In ethanol, phenyl isothiocyanate and compound 4 were dissolved. For four to five hours, the reaction mixture was allowed to boil under reflux. The product that precipitated at the end of the reaction was filtered out.

Synthesis of 2-(4-(5-mercapto-4-phenyl-4H-1,2,4-triazol-3-yl) phenyl)-1H-benz[d]imidazole-5-carbonitrile (6)

Compound 5 (0.001 mol) and NaOH (0.012 mol) solution in ethanol was refluxed under stirring for 2 h. Following the completion of the reaction, 37% HCl was added to the solution to acidify it. The precipitate was then filtered, cleaned with water, dried, and recrystallized from ethanol.

Synthesis of target compounds (7a-7e)

A suitable acetylated aniline derivative (0.001 mol), potassium carbonate (0.138 g, 0.001 mol), and a solution of compound 6 (0.001 mol) in acetone (10 ml) were refluxed at 40 $^{\circ}$ C for 12 hours. After the solvent was evaporated, the residue was cleaned with water, dried, and separated from the ethanol by recrystallization.

2-((5-(4-(5-Cyano-1H-benzo[d]imidazole-2-yl)phenyl)-4-phenyl-4H-1,2,4-triazol-3-yl)thio)-N-(3,5-dichlorophenyl)acetamide (**7a**)

Yield: 78%. Physical state: semi-solid. ¹H-NMR (400 MHz, DMSO-d₆): $\delta = 4.50$ (2H, s, CH₂), 7.14 (1H, br.s., Aromatic CH), 7.29-7.35 (3H, m, Aromatic CH), 7.59-7.60 (3H, m, Aromatic CH), 7.62 (2H, d, *J*=8.12 Hz, Aromatic CH), 7.69-7.98 (3H, m, Aromatic CH), 8.15 (2H, d, J=8.76 Hz, Aromatic CH), 11.06 (1H, s, NH). ¹³C-NMR (100 MHz, DMSO-d₆): δ(ppm): 31.16, 114.79, 115.42, 117.64, 119.87, 121.19, 121.74, 122.23, 122.58, 124.46, 125.71, 126.47, 127.17, 127.45, 129.21, 129.60, 130.37, 133.22, 135.02, 137.32, 141.35, 143.51, 147.87, 154.00, 169.30. $[M+H]^+$ 152.20, calcd C₃₀H₁₉N₇OCl₂S: 596.0822; found: 596.0833. Anal. calcd. For $C_{30}H_{19}N_7OCl_2S$, C, 60.41; H, 3.21; N,16.44. Found: C, 60.54; H, 3.20; N, 16.41.

2-((5-(4-(5-Cyano-1H-benzo[d]imidazole-2-yl)phenyl)-4-phenyl-4H-1,2,4-triazol-3-yl)thio)-N-(2,5-dichlorophenyl)acetamide (**7b**)

Yield: 79%. Physical state: semi-solid. 1 H-NMR (400 MHz, DMSO-d₆): δ = 4.50 (2H, s, CH₂), 7.12 (1H, br.s., Aromatic CH), 7.48-7.51 (3H, m, Aromatic CH), 7.61-7.66 (2H, m, Aromatic CH), 7.66-7.68 (2H, m, Aromatic CH), 7.98-7.99 (1H, m, Aromatic CH), 8.10-8.21 (3H, m, Aromatic CH), 8.38-8.41 (3H, m, Aromatic CH), 11.06 (1H, s, NH). 13 C-NMR (100 MHz, DMSO-d₆): δ (ppm): 31.16, 115.83, 116.46, 119.87, 121.33, 121.81, 124.66, 125.15, 125.87, 126.47, 126.75, 127.72, 128.14, 128.70, 129.60, 130.09, 131.48, 132.87, 134.68, 135.16, 140.18, 142.95, 149.55, 152.13, 153.73, 166.10. [M+H] $^+$ /2 calcd for C₃₀H₁₉N₇OCl₂S: 298.5451; found: 298.5447. Anal. calcd. For C₃₀H₁₉N₇OCl₂S, C, 60.41; H, 3.21; N,16.44. Found: C, 60.51; H, 3.20; N, 16.45.

2-((5-(4-(5-Cyano-1H-benzo[d]imidazole-2-yl)phenyl)-4-phenyl-4H-1,2,4-triazol-3-yl)thio)-N-(3,4-dichlorophenyl)acetamide (**7c**)

Yield: 76%. M.p. 150.2 °C. ¹H-NMR (400 MHz, DMSO-d₆): δ = 4.45 (2H, s, CH₂), 7.09 (2H, s, Aromatic CH), 7.29-7.34 (3H, m, Aromatic CH), 7.58-7.63 (2H, m, Aromatic CH), 7.72-7.79 (3H, m, Aromatic CH), 8.14-8.20 (3H, m, Aromatic CH), 8.41-8.46 (2H, m, Aromatic CH), 11.05 (1H, s, NH). ¹³C-NMR (100 MHz, DMSO-d₆): δ (ppm): 31.15, 111.73, 114.58, 116.81, 118.50, 119.24, 120.35, 120.67, 121.39, 122.65, 123.20, 125.15, 127.03, 127.51, 130.16, 130.99, 131.89, 133.42, 135.87, 136.62, 142.18, 144.41, 146.22, 151.29, 153.17, 165.20. [M+H]⁺/2 calcd for C₃₀H₁₉N₇OCl₂S: 298.5451; found: 298.5447. Anal. calcd. For C₃₀H₁₉N₇OCl₂S, C, 60.41; H, 3.21; N,16.44. Found: C, 60.53; H, 3.22; N, 16.39.

2-((5-(4-(5-Cyano-1H-benzo[d]imidazole-2-yl)phenyl)-4-phenyl-4H-1,2,4-triazol-3-yl)thio)-N-(2,6-dichlorophenyl)acetamide (**7d**)

Yield: 72 %. Physical state: semi-solid. 1 H-NMR (100 MHz, DMSO-d₆): δ = 4.48 (2H, s, CH₂), 7.13 (1H, s, Aromatic CH), 7.32-7.35 (4H, m, Aromatic CH), 7.51-7.62 (4H, m, Aromatic CH), 7.75-7.81 (1H, m, Aromatic CH), 7.80-7.95 (1H, m, Aromatic CH), 8.12-8.19 (2H, m, Aromatic CH), 8.40-8.48 (2H, m, Aromatic CH), 11.05 (1H, s, NH). 13 C-NMR (100 MHz, DMSO-d₆): δ (ppm): 31.16, 114.37, 116.95, 118.27, 118.61, 119.52, 121.19, 122.09, 122.51, 123.20, 123.76, 124.39, 124.87, 125.64, 126.75, 127.86, 129.81, 131.27, 132.52, 133.56, 141.77, 143.16, 146.50, 151.43, 153.45, 164.85.

[M+H]⁺/2 calcd for C₃₀H₁₉N₇OCl₂S: 298.5451; found: 298.5447. Anal. calcd. For C₃₀H₁₉N₇OCl₂S, C, 60.41; H, 3.21; N,16.44. Found: C, 60.35; H, 3.22; N, 16.39.

N-(4-((1H-imidazol-1-yl)methyl)phenyl)-2-((5-(4-(5-cyano-1H-benzo[d]imidazole-2-yl)phenyl)-4-phenyl-4H-1,2,4-triazol-3-yl)thio)acetamide (**7e**)

Yield: 78%. Physical state: semi-solid. 1 H-NMR (400 MHz, DMSO-d₆): δ = 4.50 (2H, s, CH₂), 5.13 (2H, s, CH₂), 6.90 (1H, s, Aromatic CH), 7.11-7.18 (2H, m, Aromatic CH), 7.30-7.35 (4H, m, Aromatic CH), 7.56-7.62 (3H, m, Aromatic CH), 7.74-7.80 (3H, m, Aromatic CH), 7.96-7.98 (1H, m, Aromatic CH), 8.12-8.23 (3H, m, Aromatic CH), 8.35-8.43 (2H, m, Aromatic CH), 11.05 (1H, s, NH). 13 C-NMR (100 MHz, DMSO-d₆): δ(ppm): 31.15, 56.50, 115.83, 117.02, 117.71, 119.77, 119.89, 121.81, 122.65, 124.32, 124.73, 125.78, 127.44, 128.11, 128.38, 128.63, 129.01, 129.08, 130.16, 130.40, 137.74, 142.25, 143.16, 143.78, 146.15, 150.46, 154.21, 166.31. [M+H]⁺/2 calcd for C₃₄H₂₅N₉OS: 304.6015; found: 304.6024. Anal. calcd. For C₃₄H₂₅N₉OS, C, 67.20; H, 4.15; N, 20.74. Found: C, 67.38; H, 4.14; N, 20.71.

Antifungal Activity

The CLSI standard technique, as outlined in the previous study [20], was used to screen the antifungal activity of the final compounds (7a-7e) against four fungal strains. Tests of the final compounds' antifungal activity were conducted using Candida albicans (ATCC 24433), Candida krusei (ATCC 6258), Candida parapsilopsis (ATCC 22019), and Candida glabrata (ATCC 9). Standard reference drugs were fluconazole (against strains of Candida) and voriconazole in this study.

Molecular docking

AutoDock VINA, which is included into the PyRx 0.8 virtual screening tool, was used to conduct docking simulations in order to assess the binding affinity [21].

In silico docking studies were conducted for the assessment of molecular interactions of compounds **7a** and **7b** with the Fungal cytochrome P450 lanosterol 14-α demethylase (CYP51) of Candida albicans (PDB:5TZ1) protein with the cocrystallised Oteseconazole (VT-1161) as the antagonist ligand. Using the UCSF Chimera Dock Prep module, protein structures were processed to guarantee an optimal structure for docking studies. This process involved removing water molecules and other ligands, adding missing atoms and residues, minimizing energy, allocating charges and polar

hydrogens, and finally converting to the pdbqt format.

ChemDraw software was used to draw the ligands' 2D structures. The structures were then optimized using the Open Babel module of PyRx's conjugate gradient algorithm and energy minimization with MMFF94 force field parameters. Finally, the ligands were transformed to the AutoDock compatible pdbqt format in order to perform docking exploration. With the aid of Chimera X and BIOVIA Discovery Studio 2021, post-docking analysis and visualization of binding positions and molecular interactions were carried out.

ADME Properties

The SWISS ADME webserver (http://www.swissadme.ch/) was used to analyze compounds 7a and 7b in order to ascertain their ADME characteristics and drug similarity [22-23].

Results and Discussion

Chemistry

The designed compounds 7a-7e were synthesized depicted in Scheme-1. In the first step, commercially available aniline derivatives were dissolved in THF at 0 °C then chloroacetyl chloride was added dropwise, and the mixture was stirred at room temperature for 1h to synthesize compounds 1a-1e. In the second step, the solution of sodium metabisulfite in ethanol was added dropwise to the 4formyl benzoate solution and was stirred at room temperature for 1h. Compound 3 was synthesized by the reaction of commercially available 5-cyano-1,2phenylenediamine with compound 2 in the presence of the catalytic amount of Na₂S₂O₅ under reflux conditions in DMF. The hydrazide derivative (compound 4) was obtained through hydrazinolysis of 4-(5-cyano-1H-benzimidazol-2-yl) benzoic acid methyl ester (3) with hydrazine hydrate. Next, phenyl isothiocyanate and compound 4 were refluxed in EtOH to obtain compound 5. Subsequently, compound 5 was cyclized with an ethanol mixture involving sodium hydroxide and then neutralized by adding concentrated hydrochloric acid to obtain 2-(4-(5-mercapto-4-phenyl-4H-1,2,4-triazol-3-yl) phenyl)-1H-benz[d]imidazole-5-carbonitrile (6). Finally, compound 6 and appropriate acetylated aniline derivatives in acetone were refluxed at 40°C for 12 h. The structures of the synthesized compounds 7a-7e were confirmed by NMR, mass and elemental analysis, and data with detailed discussions are in the experimental section.

Scheme-1: General scheme for synthesis of compounds 7a-7e.

Antifungal Activity

To determine the antifungal potential of the synthesized compounds **7a–7e**, an *in vitro* approach was employed against *C. albicans*, *C. krusei*, *C. parapsilopsis*, and *C. glabrata*. Table-1 presents the

results of the *in-vitro* study. All compounds from **7a to 7e** showed effectiveness against *C. glabrata*. The activity of these compounds **7a–7e** was comparable to reference standards with mean minimum Inhibitory Concentration values ranging from 0.97–3.90 micro gram per ml for *C. glabrata*. Compounds

7a and **7b** in particular were the most efficient ones in the series with MIC value of 0.97 micro gram per ml. The compounds **7a-7e** were found to be less effective against all other tested strains when compared with the standard reference compounds voriconazole and fluconazole.

Table-1: Antifungal activity of the compounds **7a-7e** as MIC values (μ g/mL).

Comp.	A	В	С	D
7a	31.25	125	0.97	31.25
7b	31.25	62.5	0.97	15.625
7c	31.25	62.5	1.95	15.625
7d	62.5	125	3.90	31.25
7e	62.5	125	1.95	31.25
S. D 1.	3.90	3.90		
S. D 2.	7.81	7.81		

*: Most active compounds. A: C. albicans (ATCC 24433), B: C. krusei (ATCC 6258), C: C. glabrata (ATCC 9), D: C. parapsilosis S.D 1. (Standard Drug 1): Voriconazole, S.D 2. (Standard Drug2): Fluconazole

Molecular docking

The compounds' molecular interactions and their binding energies were contrasted with the Oteseconazole, a co-crystallized ligand of Lanosterol 14α-demethylase and Fluconazole and Voriconazole which were used as standards for *in vitro* antifungal activity. The binding energy plot of compounds **7a**, **7b**, Oteseconazole, Fluconazole and Voriconazole containing fungal CYP51 is given in Fig 1. The results of studies are following:

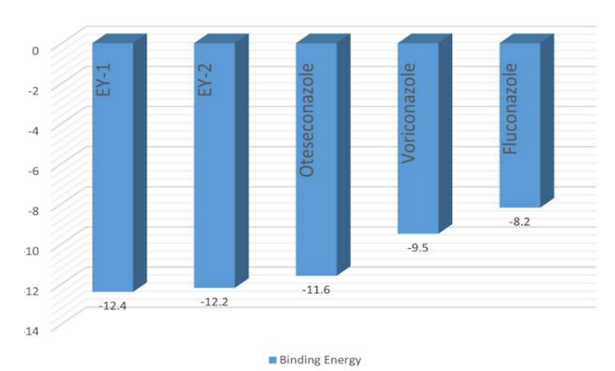


Fig. 1: Binding energy plot of compounds 7a, 7b, Oteseconazole, Fluconazole and Voriconazole with fungal CYP51.

Analysis of compounds' molecular interaction with CYP51

The interaction summary of compounds 7a, 7b, Oteseconazole, Voriconazole and Fluconazole is shown in Table-2. Compound **7a** (3,5 dichloro analogue) showed better interaction profile compared with the other analogue **7b** (2,5 dichloro analogue) and standard antifungal agents (Oteseconazole, Fluconazole and Voriconazole). Its binding energy was -12.4 Kcal/mol with one hydrogen bond interaction with critical active site residue of TYR132 through the triazole heterocyclic ring's nitrogen atom

located centrally in the scaffold. Benzimidazole ring in this compound had a pi-pi interaction with HIS377 and PHE233 whereas the residue TYR118 also plays role in the similar pi-pi interaction with the triazole ring and then the phenyl substituent at the 5th position of the triazole had pi-sulfur interactions with MET508 and the same residue also had pi-alkyl interactions with the other phenyl substitution at the 4th position of the triazole ring. ILE131 and ILE304 residues participate in the pi-alkyl interactions with the phenyl ring with 3,5 dichloro substitutions and PRO230 also had pi-alkyl interactions with benzimidazole ring. Moieties at the 3rd position of the triazole ring (Sulfanyl N-(3,5 dichloro phenyl) acetamide) had diverse type of interactions with Haem ring of the cytochrome like pi-sigma with acetamide and pi-sulfur interaction with sulfanyl and then pi-pi T shaped and pi-alkyl interactions with dichloro substituted phenyl ring of 7a and it interacted with the other amino acids in the active site via van der Waals forces.

Compound 7b had a binding energy of -12.2 Kcal/mol which is in close range with the binding energy of 7a due to structural similarly with the only difference in the position of the halogen (-Cl). Compound 7b also had similar H-bond interaction with TYR132 like 7a but the moiety contributing to this interaction is -C=O of the acetamide moiety in compound 7b whereas the triazole ring's nitrogen atom is responsible for the hydrogen bond interaction with compound 7a. It also had other H-bonding interaction with SER507 through the nitrogen of the benzimidazole ring. PHE228 participate in the pi-pi interaction with the phenyl ring at the 4th position of triazole ring whereas the HIS377 had a pi-pi Tshaped interaction with the benzimidazole rings. MET508 had pi-sulphur interaction with the phenyl substituted moiety on the triazole at 4th position and Similar pi-sulphur interactions of sulfanyl group affixed to the triazole ring's third position was observed with residues like TYR132 and PHE126. Ph-sigma interactions were displayed by LEU376 and ILE131 with unsubstituted phenyl ring and dichloro substituted phenyl ring respectively. Additionally, a number of pi-alkyl interactions with residues were noted like ILE304, LYS143, LEU139, LEU121 and PRO230 with the aromatic rings in the EY2 scaffold. Haem ring is interacting mainly through the pi-sigma and pi-alkyl interactions. Vander Waals interactions were present in the nearby active site residues. 2D molecular interactions of compounds 7a (A), 7b (B), Fluconazole (C), Voriconazole (D) and Oteseconazole are given in Fig 2.

Table-2: Interaction summary of compounds 7a, 7b, Oteseconazole, Voriconazole and Fluconazole.

Compounds	Binding Energy (K.cal/mol)	Fungal Lanosterol 14-a demethylase (CYP15)
7a	-12.4	TYR132, TYR118, LEU376, HIS377, PHE233, MET508, PRO230, ILE131, ILE304, SER506
7b	-12,2	TYR132, SER507, LEU376, ILE131, HIS377, PHE228, MET508, PRO230, LEU121, ILE304, LEU139,
		LYS143
Oteseconazole	-11.6	TYR132, PHE233, MET508, HIS377, LEU376, LEU121, PRO230, ILE131, ILE304
Voriconazole	-9.5	TYR132, TYR118, PHE228,LEU376, TYR118, LEU121
Fluconazole	-8.2	TYR118, ILE131, LEU376, MET508, VAL509, GLY307

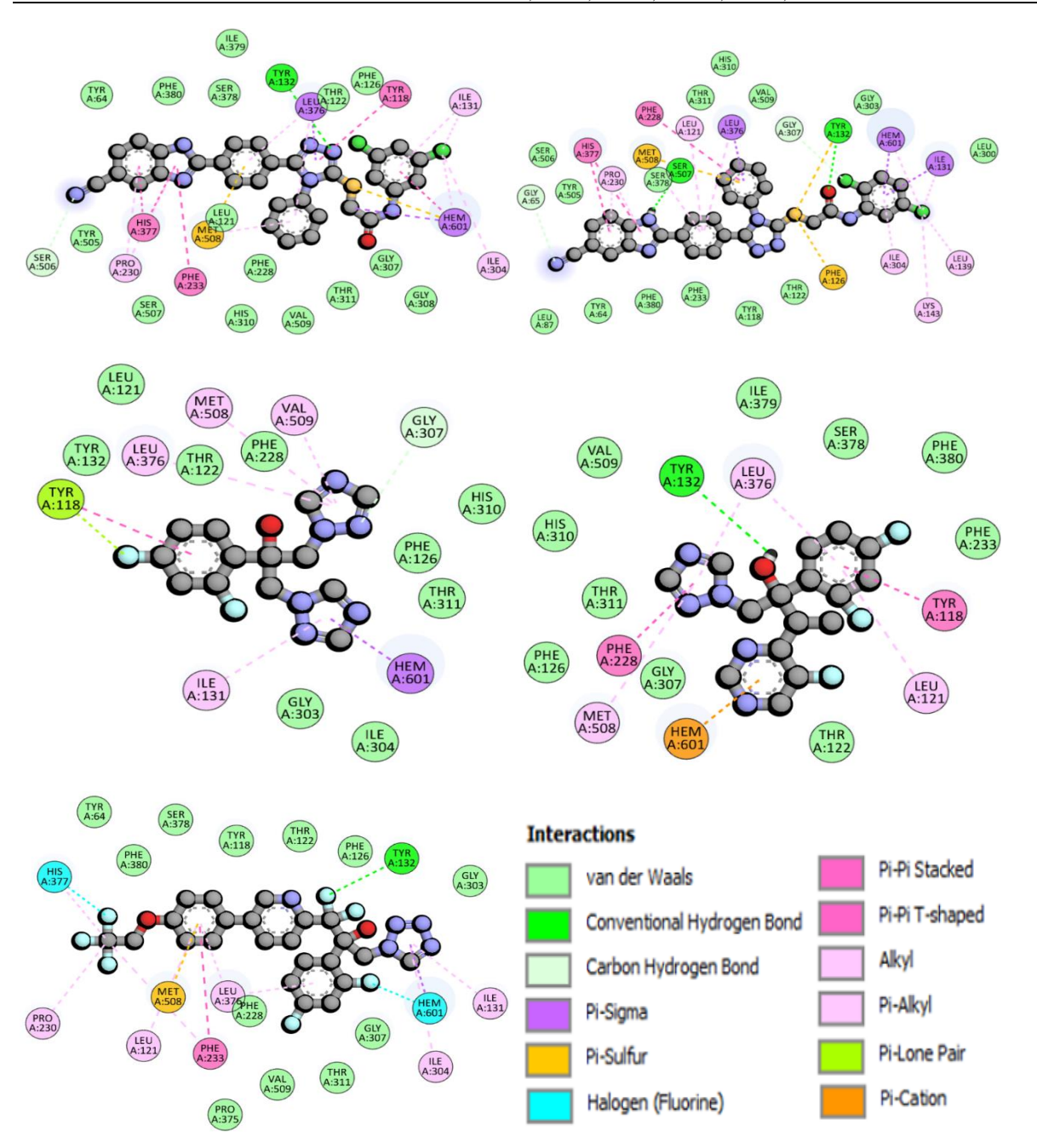


Fig 2: 2D molecular interactions of compounds 7a (**A**), 7b (**B**), Fluconazole (**C**), Voriconazole (**D**) and Oteseconazole (**E**) with the critical amino acid residues of the fungal cytochrome P450 lanosterol $14-\alpha$ demethylase protein. Interactions were displayed as colour coded dashed lines; green lines indicated the H–bonds.

The docking program was validated through the re-docking of Oteseconaole (VT1161 or VT1) into its co-crystallized binding site. Between the docked (cyan) and native (grey) poses, the lower Root Mean Square Deviation (RMSD) value of 1.77 Å indicates how accurately the algorithm predicted the binding shape of oteseconazole.

Oteseconazole is the co-crystallized ligand with several halogen substitutions (-F) and among them a fluoro group had a H-bond interaction with TYR132 which is the residue involved in the H-bond interactions with both compounds 7a and 7b and this is a common hydrogen bond interaction in all these three compounds and interaction with this critical residue might be holding a potential in modulating the protein for antifungal action. Next to the trifluoro ethoxy group, PHE233 exhibited a pi-pi stacking contact with the phenyl group, while MET508 exhibited a pi-sulphur interaction with the same phenyl ring. PRO230, LEU121, ILE304, ILE31 residues are involved in alkyl and pi-alkyl interactions with the sidechain and aromatic rings in the scaffold of the compound. HIS377 had halogen interactions with the fluoro group apart from the hydrophobic alkyl interactions with ethoxy linker moiety. Haem ring at the protein's active site had halogen interactions with one of the fluoro group on the difluoro phenyl ring and it also had pi-sigma and pialkyl interactions with the nearby tetrazole ring and other active site residues had Vander waals interactions.

Voriconazole and Fluconazole are the triazole standard antifungal agents considered to have an assessment of their binding energy and interactions to compare with the compounds **7a** and **7b** due to their promising bioactivity against the fungal growth.

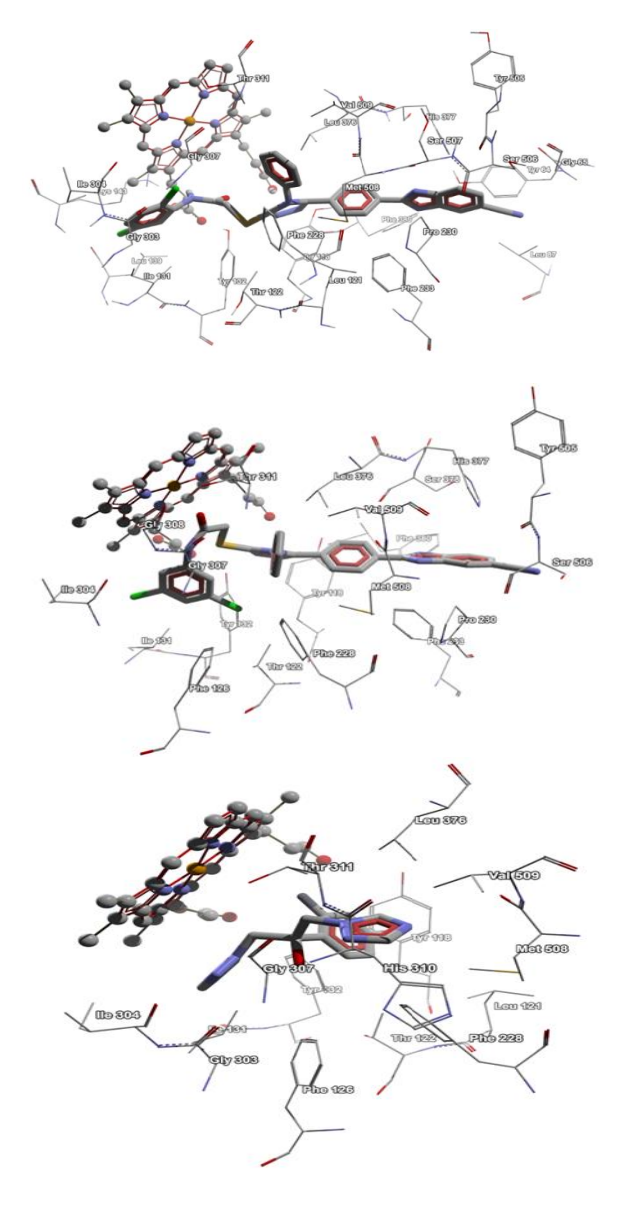
Voriconazole had a binding energy of -9.5 Kcal/mol and displaying a Hydrogen bond with TYR132 residue where the -OH group of the butanol linking various aromatic and heterocyclic rings like triazole is contributing to this hydrogen bond interaction. PHE228 had a pi-pi stacked interaction, MET508 and LEU376 had pi-alkyl interactions with the triazole ring. LEU376 also had the similar pi-alkyl interactions with the aromatic ring with difluoro substitution along with the residue LEU121 and then with the same aromatic ring, TYR118 exhibited a pi-pi T-shaped interaction. Haem had pi-cation interactions with pyrimidine aromatic ring.

The binding energy of fluconazole is -8.2 Kcal per mol and it showed a non-hydrogen interactions with the CYP51's active site. It exhibited pi-pi T-shaped and pi-lone pair interactions with TYR118. LEU376,

MET508, VAL509 and ILE131 had pi-alky interactions with triazole rings.

TYR132 and TYR118 are the residues that had H-bonds with the propionates in the haem cytochrome [24] and disrupting those crucial interactions through the formation of novel H-bond interactions with TYR132 in the case of compounds **7a**, **7b**, Oteseconazole and Voriconazole are the significant interactions which might help us to decipher the mechanism of their probable antifungal activity through structural perspective of CYP51.

Overall compounds **7a** and **7b** showed good molecular interaction profile for CYP51. Their biding pattern and respective alignment in the active site are depicted in Figs 3-4, respectively.



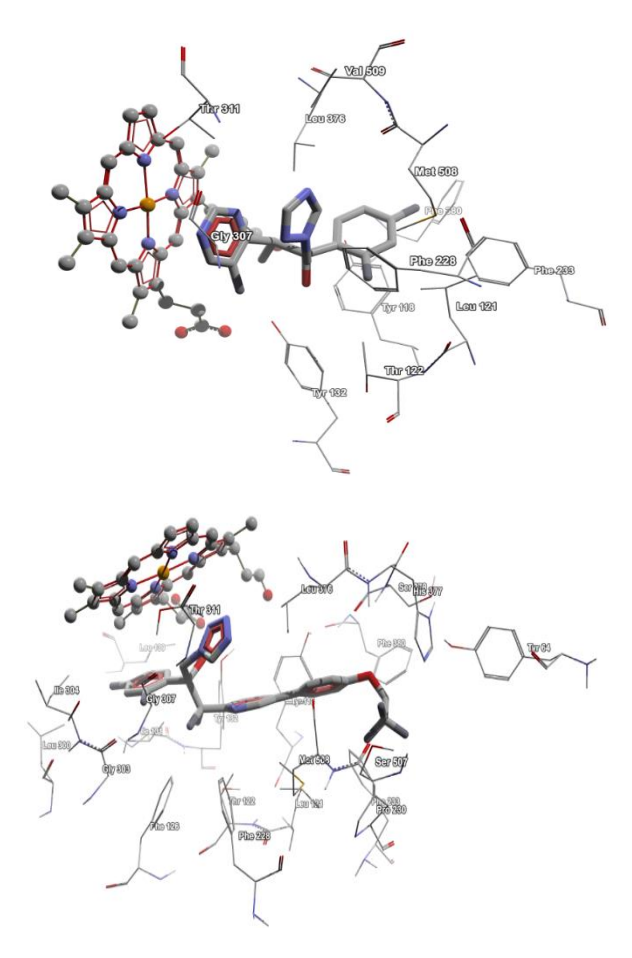


Fig. 3: 3D representation of compounds' 7a (A), 7b (B), Fluconazole (C), Voriconazole (D) and Oteseconazole (E) binding poses in the active residue of fungal CYP51 exhibiting the proximity of critical amino acid residues of the protein.

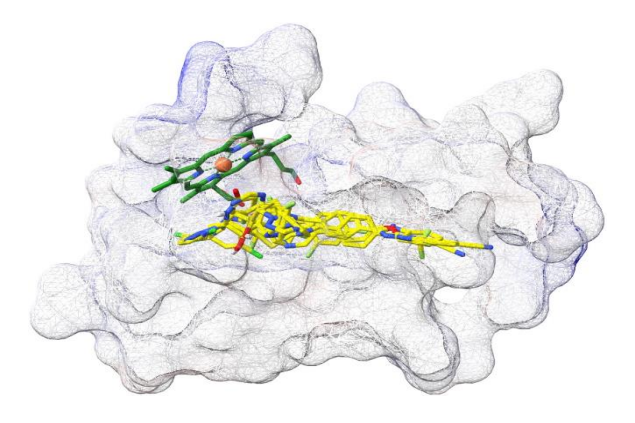


Fig. 4: Molecular alignment of binding poses of compounds in the active site pocket of fungal CYP51 with Haem represented in green and compounds represented in yellow colour.

Pharmacophore models were developed using ZINCPharmer and the common Pharmacophore features of all the five compounds (7a, 7b, Oteseconazole, Voriconazole and Fluconazole) can be visualized in the **Fig 5**, the pharmacophoric features were represented as spheres with different colours in the following way: Hydrophobic (green), aromatic (purple), H-bond donors (white) and acceptors (orange). Overlap of various features between the compounds **7a**, **7b** and the standard antifungal agents indicates that these compounds hold the potential to orient and display similar interactions with critical residues (TYR132) which might be translating into a potential activity.

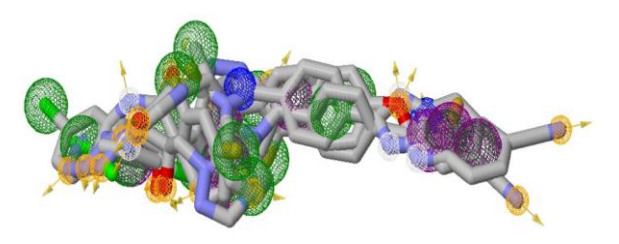


Fig. 5: Pharmacophore features of compounds following molecular alignment of binding poses in the active site pocket of fungal CYP51.

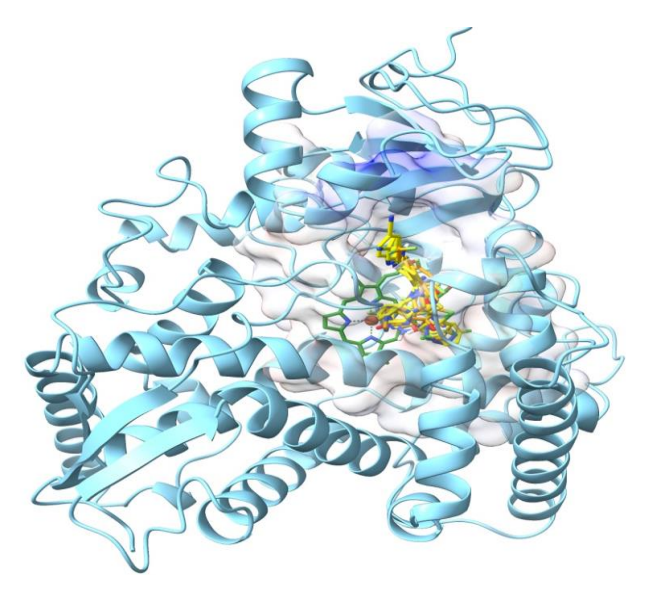
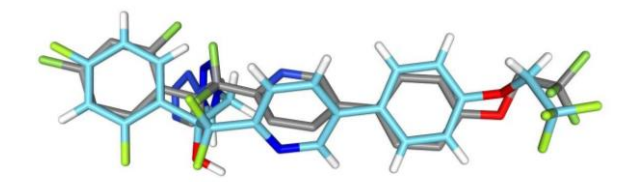


Fig. 6: Ribbon representation of the Fungal CYP51 protein demonstrating the binding site of compounds with Haem and compounds are represented in green and yellow colours respectively.

Binding site of the compounds in the CYP51 along with Haem of the cytochrome can be viewed

from the Fig 6. The alignment of native and docking poses of VT1 after re-docking is given in Fig 7.



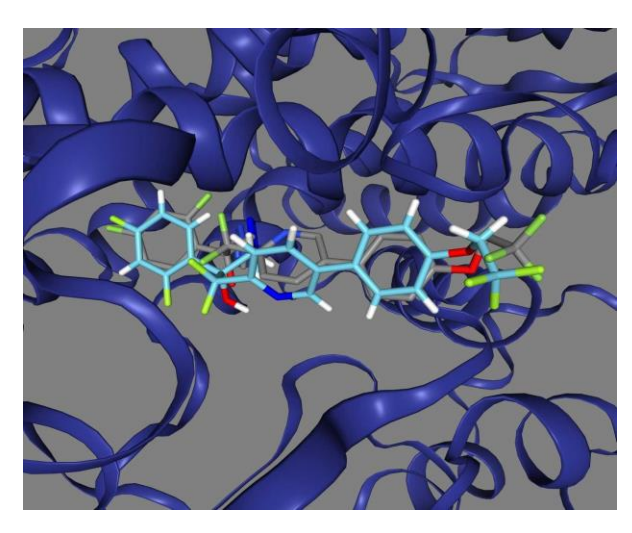


Fig 7: Alignment of native and docking poses of VT1 following the re-docking.

Table-3: Physico-chemical characteristics and druglikeness predictions of compounds using Swiss ADME model.

Parameters	7a & 7b	
Molecular Weight (g/mol)	596.49	
Log P o/w	5.73	
No of H-bond Donors	2	
No of H-bond Acceptors	5	
Solubility	Poor	
TPSA	137.58	
GI absorption	Low	
BBB permeation	No	
P-gp substrate	No	
Drug likeness (Lipinski)	No	
Bioavailability score	0.17	
CYP450 isoforms inhibition	CYP2C19, CYP3A4	

ADME Properties

the SWISS ADME Using website (http://www.swissadme.ch/), compounds 7a and 7b were analysed to ascertain their **ADME** characteristics and drug likeness. Physico-chemical properties of the compounds are given in Table 3. Similar predictions were made because of their close structural resemblance, with the exception of a minor change in the chlorine's location. The findings showed that the compound's Lipinski resemblance deviates slightly depending

its weight and Log P. The chemicals were not recognized as P-glycoprotein (P-gp) substrates and were anticipated to have no BBB penetration. The CYP2C19 and CYP3A4 isoforms may be inhibited by these substances. They have weak solubility and low gastrointestinal absorption, according to their pharmacokinetic features. These results imply that additional optimization is necessary to improve the compounds' biopharmaceutical qualities in subsequent research.

Conclusion

A series of benzimidazole-triazoles was designed and synthesized in this article because of our interest in the rational design of 14α -demethylase inhibitors. In comparison to the reference drugs fluconazole and voriconazole, all compounds showed promising inhibitory effects against C. glabrata lanosterol 14α -demethylase enzyme with MIC₅₀ values of 0.97-3.90 µg/ml. Notably, the compounds showed poor interactions and the least amount of antifungal activity against C. albicans, C. krusei, and C. parapsilopsis, which accounts for their low potency. MD analyses demonstrated that 7a and 7benzyme interactions were persistent over the course of the simulation and actively participated in the demethylase active site through a number of H-bound interactions. Computed physicochemical ADMET parameters demonstrated the derived compounds' druggability. These results will have a significant impact on the structural layout of 14αdemethylase inhibitors for designing new anti-fungal compounds.

References

- E. Vitaku, D.T. Smith, and J.T. Njardarson, Analysis of the structural diversity, substitution patterns, and frequency of nitrogen heterocycles among US FDA approved pharmaceuticals: miniperspective, *J. Med. Chem.*, 57, 10257 (2014).
- 2. M. Frieri, K. Kumar, and A. Boutin, Antibiotic resistance, *J. Infect. Public Health.*, **10**, 369 (2017).
- L. Kumari, A. Mazumder, D. Pandey, M.S. Yar, R. Kumar, R. Mazumder, M. Sarafroz, M.J. Ahsan, V. Kumar, and S. Gupta, Synthesis and biological potentials of quinoline analogues: A review of literatüre, *Mini-Rev. Org. Chem.*, 16, 653 (2019).
- B.S. Matada, R. Pattanashettar, and N.G. Yernale, A comprehensive review on the biological interest of quinoline and its

- derivatives, *Bioorg. & Med. Chem.*, **32**, 115973 (2021).
- S. Salahuddin, and A. Mazumder, Benzimidazoles: A biologically active compounds, *Arabian J. Chem.*, 10, S157 (2017).
- D. Diaconu, D. Amăriucăi-Mantu, V. Mangalagiu, V. Antoci, G. Zbancioc, and II. Mangalagiu, Ultrasound assisted synthesis of hybrid quinoline-imidazole derivatives: a green synthetic approach, RSC adv., 11, 38297 (2021).
- D. Diaconu, V. Mangalagiu, D. Amariucai-Mantu, V. Antoci, C.L. Giuroiu, and II. Mangalagiu, Hybrid quinoline-sulfonamide complexes (M2+) derivatives with antimicrobial activity, *Molecules.*, 25, 2946 (2020).
- 8. O. Ebenezer, F. Oyetunde-Joshua, O.D. Omotoso, and M. Shapi, Benzimidazole and its derivatives: Recent Advances (2020-2022), *Res. Chem.*, 100925 (2023).
- 9. E. Kabir, and M. Uzzaman, A review on biological and medicinal impact of heterocyclic compounds, *Res. Chem.*, 100606 (2022).
- S. Tahlan, S. Kumar, and B. Narasimhan, Antimicrobial potential of 1H-benzo [d] imidazole scaffold: a review, *BMC Chem.*, 13, 1 (2019).
- F.V. Lopes, P. H. F. Stroppa, J.A. Marinho, R.R. Soares, L. de Azevedo Alves, P.V.Z.C. Goliatt, C. Abramo, and A.D. da Silva, 1,2,3-Triazole derivatives: Synthesis, docking, cytotoxicity analysis and in vivo antimalarial activity, *Chem-Biol. Interact.*, 350, 109688 (2021).
- 12. S.A. El-Sebaey, Recent Advances in 1,2,4-Triazole Scaffolds as Antiviral Agents, *ChemistrySelect.*, **5**, 11654 (2020).
- 13. R.J. Brüggemann, R. Verheggen, E. Boerrigter, M. Stanzani, P.E. Verweij, N.M. Blijlevens, and R.E. Management of drug-drug Lewis, of targeted therapies interactions for haematological malignancies and triazole antifungal drugs, Lancet. Haematol., **9**, e58 (2022).
- 14. Bozorov, K., Zhao, J., and Aisa, H.A., 1,2,3-Triazole-containing hybrids as leads in medicinal chemistry: A recent overview, *Bioorg. Med. Chem.*, 27, 3511 (2019).
- A.G.S. Warrilow, C.M. Hull, J.E. Parker, E. P. Garvey, W. J. Hoekstra, W. R. Moore, R. J. Schotzinger, D. E. Kelly, and S. L. Kelly, The clinical candidate VT-1161 is a highly potent

- inhibitor of Candida albicans CYP51 but fails to bind the human enzyme, *Antimicrob. Agents Chemother.*, **58**, 7121 (2014).
- 16. M. Keenan, and J.H. Chaplin, A new era for Chagas disease drug discovery?, *Prog. Med. Chem.*, **54**, 185 (2015).
- 17. N.Ö. Can, U. Acar Çevik, B.N. Sağlık, S. Levent, B. Korkut, Y. Özkay, Z.A. Kaplancıklı, and A.S. Koparal, Synthesis, molecular docking studies, and antifungal activity evaluation of new benzimidazole-triazoles as potential lanosterol 14α-demethylase inhibitors, *J. Chem.* (2017).
- H. Karaca Gençer, U. Acar Çevik, S. Levent, B.N. Sağlık, B. Korkut, Y. Özkay, S. Ilgın, and Y. Öztürk, New benzimidazole-1,2,4-triazole hybrid compounds: Synthesis, anticandidal activity and cytotoxicity evaluation, *Molecules.*, 22, 507 (2017).
- E. Güzel, U. Acar Çevik, A.E. Evren, H.E. Bostancı, Ü.D. Gül, U. Kayış, Y. Özkay, and Z.A. Kaplancıklı, Synthesis of benzimidazole-1,2,4-triazole derivatives as potential antifungal agents targeting 14α-demethylase, ACS omega., 8, 4369 (2023).
- U.A. Çevik, I. Celik, A. Işık, R.R. Pillai, T.E. Tallei, R. Yadav, Y. Özkay, and Z.A. Kaplancıklı, Synthesis, molecular modeling, quantum calculations and ADME estimation studies of benzimidazole-oxadiazole derivatives as potent antifungal agents, J. Mol. Struct., 1252, 132095 (2022).
- 21. S. Dallakyan, and A.J. Olson, Small-molecule library screening by docking with PyRx, *Chem. Biol: Methods Protoc.*, 243 (2015).
- 22. A. Daina, O. Michielin, and V. Zoete, SwissADME: a free web tool to evaluate pharmacokinetics, drug-likeness and medicinal chemistry friendliness of small molecules, *Sci. Rep.*, **7**, 42717 (2017).
- 23. D.R. Koes, and C.J. Camacho, ZINCPharmer: pharmacophore search of the ZINC database, *Nucleic acids res.*, **40**, W409 (2012).
- 24. T.Y. Hargrove, L. Friggeri, Z. Wawrzak, A. Oi, W.J. Hoekstra, R.J. Schotzinger, J.D. York, F.P. Guengerich, and G.I. Lepesheva, Structural analyses of Candida albicans sterol 14α-demethylase complexed with azole drugs address the molecular basis of azole-mediated inhibition of fungal sterol biosynthesis, *J. Biol. Chem.*, 292, 6728 (2017).